DOI 10.5012/bkcs.2010.31.11.3283

Gas-phase Dehydration of Glycerol over Supported Silicotungstic Acids Catalysts

Yong Tae Kim, Kwang-Deog Jung,† and Eun Duck Park*

*Division of Energy Systems Research and Division of Chemical Engineering and Materials Engineering, Ajou University, Suwon 443-749, Korea. *E-mail: edpark@ajou.ac.kr*
†Clean Energy Research Center, Korea Institute of Science and Technology, Cheongryang, P. O. Box 131, Seoul 136-791, Korea
Received August 17, 2010, Accepted September 14, 2010

The gas-phase dehydration of glycerol to acrolein was carried out over 10 wt % HSiW catalysts supported on different supports, *viz*. γ-Al_2O_3, SiO_2-Al_2O_3, TiO_2, ZrO_2, SiO_2, AC, CeO_2 and MgO. The same reaction was also conducted over each support without HSiW for comparison. Several characterization techniques, N_2-physisorption, thermogravimetric analysis (TGA), differential scanning calorimetry (DSC), the temperature-programmed desorption of ammonia (NH_3-TPD), temperature-programmed oxidation (TPO) with mass spectroscopy and CHNS analysis were employed to characterize the catalysts. The glycerol conversion generally increased with increasing amount of acid sites. Ceria showed the highest 1-hydroxyacetone selectivity at 315 °C among the various metal oxides. The supported HSiW catalyst showed superior catalytic activity to that of the corresponding support. Among the supported HSiW catalysts, HSiW/ZrO_2 and HSiW/SiO_2-Al_2O_3 showed the highest acrolein selectivity. In the case of HSiW/ZrO_2, the initial catalytic activity was recovered after the removal of the accumulated carbon species at 550 °C in the presence of oxygen.

Key Words: Dehydration, Glycerol, Acrolein, Silicotungstic acids, Acidity

Introduction

The conversion of biomass into chemicals has attracted much attention because biomass can replace fossil resources and it is ultimately free from CO_2 emission. Therefore, the use of glycerol, which is the main byproduct during the synthesis of biodiesel, is a welcome advance.[1] Through its dehydration, glycerol can be converted into acrolein, which is a key intermediate in the synthesis of acrylic acid, acrylic acid esters, superabsorber, polymers and detergents.[2] Acrolein is traditionally produced through the partial oxidation of propylene over mixed metal oxides containing Bi-Mo(W)-O phase.[3] For the synthesis of acrolein from glycerol, acid catalysts should be used to selectively protonate its hydroxyl groups.

Various acid catalysts have been examined for this reaction in either the liquid or gaseous phase.[4-32] In the liquid-phase reaction, various homogeneous and heterogeneous acid catalysts, *viz*. bezenesulfonic acid,[4] sulfonic acid,[5] metal phosphates,[7] alumina,[9] zeolite[9] and metal sulfates,[10] have been investigated. However, most homogeneous catalysts have some drawbacks, such as their high toxicity, corrosiveness and the large quantity of waste water. Moreover, the glycerol conversion should be kept low in order to increase the acrolein selectivity in the liquid-phase reaction.[11]

The gas-phase reaction has been investigated to achieve a high acrolein selectivity with a high glycerol conversion. Various solid acid catalysts, *viz*. metal phosphates,[8,9,13-16] metal sulfates,[17] metal oxides,[17-19] supported heteropolyacids (HPAs)[17,20-26] and zeolites,[11,17,27,28-32] have been reported.

HPAs with well defined Keggin structures are well-known solid acid catalysts. They have been commercially applied to several petrochemical processes, because they have stronger Brönsted acid sites than conventional solid acid catalysts such as SiO_2-Al_2O_3 and zeolites.[33] The acid strength of crystalline HPAs generally decreases in the following order: HPW ($H_3PW_{12}O_{40}\cdot xH_2O$) > HSiW ($H_4SiW_{12}O_{40}\cdot xH_2O$) >> HPMo ($H_3PMo_{12}O_{40}\cdot xH_2O$) > HSiMo ($H_4SiMo_{12}O_{40}\cdot xH_2O$).[34] It was reported that among the various silica-supported HPAs, HSiW/SiO_2 showed the most stable catalytic activity for the dehydration of glycerol and was also resistant to water vapor.[20]

In this work, we chose HSiW as the heteropolyacid and examined the effect of the support on the gas-phase dehydration of glycerol over the supported HSiW. The catalytic activity of the corresponding support was also investigated for the purpose of comparison.

Experimental

Preparation of catalysts. Various supports, *viz*. γ-Al_2O_3 (Strem Chem.), SiO_2-Al_2O_3 (SiO_2/Al_2O_3 = 7.4, Sigma-Aldrich), TiO_2 (P25, Degussa), SiO_2 (Merck), AC (Sigma-Aldrich) and CeO_2 (Rhodia) were purchased and utilized as a support or a catalyst. Additionally, ZrO_2 was prepared from $ZrCl_2O\cdot 8H_2O$ (Junsei Chemical Co.) by the precipitation method using ammonia solution as a precipitant. MgO (Yakuri Pure Chem.) was hydrothermally treated in water at 60 °C for 6 h to increase the BET surface area. The precipitates were dried at 120 °C overnight and calcined in air at 500 °C.

Silicotungstic acid ($H_4SiW_{12}O_{40}\cdot xH_2O$, HSiW) was purchased from Alfa Aesar and used as a precursor for the preparation of supported HSiW catalysts by the wet impregnation method. The support was added to aqueous solutions containing a prescribed amount of HSiW and the slurry was stirred at 60 °C for 6 h. The excess water was removed with a rotary evaporator at 60 °C and dried in an oven at 120 °C overnight. The content of HSiW was intended to be 10 wt % for all of the supported HSiW catalysts. The physical properties of all of the catalysts are listed in table (Supplementary Table 1). All of the catalysts were

Table 1. The NH_3-TPD results for the supports and supported HSiW catalysts

Catalysts	NH_3-TPD peak position (°C)		Acid amount (mmol $NH_3/g_{cat.}$)[a]		
	Low-temperature region	High-temperature region	Total	Low-temperature region	High-temperature region
TiO_2	230	-	8.0×10^{-2}	8.0×10^{-2}	0
ZrO_2	239	-	9.0×10^{-2}	9.0×10^{-2}	0
SiO_2	-	-	0	0	0
AC	-	-	0	0	0
CeO_2	211	385	1.8×10^{-1}	9.0×10^{-2}	9.0×10^{-2}
MgO	-	-	0	0	0
HSiW/γ-Al_2O_3	230	332	2.7×10^{-1}	1.3×10^{-1}	1.4×10^{-1}
HSiW/SiO_2-Al_2O_3	226	327	5.3×10^{-1}	2.0×10^{-1}	3.3×10^{-1}
HSiW/TiO_2	224	309	1.0×10^{-1}	4.0×10^{-2}	6.0×10^{-2}
HSiW/ZrO_2	220	301	1.4×10^{-1}	4.0×10^{-2}	9.0×10^{-2}
HSiW/SiO_2	212	268	7.0×10^{-2}	5.0×10^{-2}	2.0×10^{-2}
HSiW/AC	215	278	1.6×10^{-1}	7.0×10^{-2}	9.0×10^{-2}
HSiW/CeO_2	230	295	2.5×10^{-1}	1.2×10^{-1}	1.3×10^{-1}
HSiW/MgO	211	-	4.0×10^{-2}	4.0×10^{-2}	0

[a]The total acidity was determined by quantifying the desorbed NH_3.

pretreated in air at 400 °C for 3 h and purged in He for 1 h before the reaction.

Characterization of catalysts. The BET surface area was calculated from the N_2 adsorption data that were obtained using an Autosorb-1 apparatus (Quantachrome) at liquid N_2 temperature. Before the measurement, the sample was degassed in a vacuum for 4 h at 200 °C. The Keggin-anion density, the number of Keggin anion dispersed on the surface of support, were calculated according to the following equation.[24]

$$Keggin-anion\ density\ (nm^{-2}) = \frac{HPA\ loading\ (wt.\%/100) \times 6.02 \times 10^{23}\ (mol^{-1})}{BET\ area\ (nm^2/g) \times FW_{HPA}\ (g/mol)}$$

The bulk crystalline structures of the catalysts were determined by the X-ray diffraction (XRD) technique. The XRD patterns were obtained with a Rigaku D/MAC-III using Cu Kα radiation (λ = 0.15406 nm) operated at 50 kV and 30 mA (1.5 kW). The assignment of the crystalline phases was carried out using PCPDFWIN software (version 2.2) for the ICDD database.

Thermogravimetric analysis (TGA) and differential scanning calorimetry (DSC) were conducted using a Simultaneous Thermal Analyser-Mass Spectrometer (STA 409pc + QMS 403c, NETZSCH) to measure the thermal change of the supported HSiW catalysts from 30 °C to 900 °C at a heating rate of 10 °C/min in air. In the case of the HSiW/AC catalyst, the TGA and DSC experiment were carried out in N_2 to prevent the oxidation of carbon.

The temperature-programmed desorption of NH_3 (NH_3-TPD) was conducted over 0.10 g of each sample from 150 to 600 °C at a heating rate of 5 °C/min while monitoring the thermal conductivity detector (TCD) signals (Autochem 2910 unit, Micromeritics) and on-line mass spectrometer signals (QMS 200, Pfeiffer Vacuum) after saturation with NH_3 at 150 °C for 30 min and then the catalysts were flushed with He at 150 °C for 1 h. For the support itself, the samples were treated in He at 600 °C for 1 h before the experiment to remove any adsorbed water or organic species. All of the supported HSiW catalysts were treated in He at 400 °C for 1 h before the experiment. All of the detected TCD peaks were deconvoluted at different maximum peak temperatures using the Peakfit 4.01 program, with a multiple Gaussian function for fitting and the area of each peak was calculated. The peak area can be correlated with the amount of adsorbed NH_3 based on the pulsed NH_3 injection experiment.

The temperature-programmed oxidation (TPO) was conducted over 0.05 g of the sample in a 2% O_2/He stream by heating the sample from 30 °C to 800 °C at a heating rate of 10 °C/min while monitoring the TCD signals (AutoChem 2910 unit, Micromeritics) and on-line mass spectrometer signals (QMS 200, Pfeiffer Vacuum) after the samples were purged with He at RT for 1 h.

The amounts of carbon and hydrogen formed on the used catalysts were determined with a CHNS analyzer (Vario EL III) after the samples were pretreated with He at 300 °C to remove any weakly chemisorbed organic compounds before the carbon analysis.

Catalytic activity tests. The dehydration of glycerol was conducted in a continuous small fixed-bed reactor with the catalysts that had been retained between 45 and 80 mesh sieves at atmospheric pressure. For the screening tests, 0.30 g of the catalyst without diluents was contacted with a standard gas consisting of 8.3 mol % $C_3H_8O_3$ and 76.3 mol % H_2O in He at atmospheric pressure. The molar flow rate of glycerol was controlled to be 23.4 mmol/h by means of a high pressure liquid chromatography (HPLC) pump (GILSON 305). The catalytic activity was measured under isothermal conditions at 315 °C.

In all cases, all of the reactants were preheated to at least 265 °C to prevent their partial condensation. For each set point, the products were collected in a cold trap maintained at −5 °C. The products in the cold trap were gathered every 2 h for an-

alysis. They were filtered with a 0.2 μM membrane filter and analyzed with a gas chromatograph equipped with an HP-FFAP column and a flame ionization detector (FID). The quantification of the products was carried out using 1-butanol in water as an external standard.

The glycerol conversion and molar carbon selectivity were quantified according to the following equations:

$$\textit{Glycerol conversion}\ (\%) = \frac{n_{Feed,i} - n_{Feed,o}}{n_{Feed,i}} \times 100$$

$$\textit{Molar carbon selectivity}\ (\%) = \frac{n_{Prod.,o}}{n_{Feed,i} - n_{Feed,o}} \times 100$$

where $n_{Feed,i}$ and $n_{Feed,o}$ are the number of moles of carbon in glycerol at the input and output, respectively; $n_{Prod.,o}$ is the number of moles of carbon in the product at the output.

Results and Discussion

The bulk crystalline structure for all of the supports and supported HSiW catalysts was probed with the XRD technique. Each support showed the typical XRD peak representing its inherent structure. None of the supported HSiW catalysts showed any XRD peaks corresponding to the HSiW Keggin structure. This implies that HSiW exists as highly dispersed species on the support. Kozhevnikov reported that the crystalline HPA phase could be observed for silica-supported HPA when the HPA loading on silica (S_{BET} = 200 - 300 m^2/g) was 30 - 50%.[35]

The Keggin-anion density of HSiW on the support was calculated and listed in table (Supplementary Table 1). The calculated surface density decreased in the following order: HSiW/TiO_2 > HSiW/ZrO_2 > HSiW/MgO > HSiW/γ-Al_2O_3 > HSiW/CeO_2 > HSiW/SiO_2 > HSiW/SiO_2-Al_2O_3 > HSiW/AC. It is well known that the thermal stability of heteropolyacids is dependent on the support and is important for the gas-phase reaction. To prevent their thermal decomposition, the interaction between the HPAs and support is important. The heteropolyacids are irreversibly decomposed through a complex multistage process with increasing temperature. The thermal stability is generally determined by the thermal analytical method including thermogravimetric analysis (TGA) and differential scanning calorimetry (DSC). The TGA results for HSiW and the supported HSiW catalysts are obtained (Supplementary Figure 1). A significant weight loss was observed in the temperature range from 30 to 900 °C. For bulk HSiW, three different decomposition peaks were observed. Among the supported HSiW catalysts, the ZrO_2- and TiO_2-supported HSiW catalysts showed the best thermal stability.

The DSC results for HSiW and the supported HSiW catalysts are shown in Fig. 1. The DSC curves for all of the tested catalysts showed an endothermic peak at ~100 °C which is due to the desorption of physisorbed water.[34] This peak intensity is dependent on the amount of hydration water in the sample. For bulk HSiW, the second endothermic peak at a temperature of around 241 °C is due to the removal of water from the hydrated heteropolyacid.[36] Atia *et al.* reported that the exothermic peak at ~540 °C in the DTA results was due to the decomposition of HSiW into WO_3(Si).[21] The DSC plots for the supported HSiW catalysts also showed exothermic peaks in the range from 462 to 586 °C that represented the decomposition of HSiW on the support. Therefore, it is worth mentioning that all of the supported HSiW catalysts are thermally stable under the reaction conditions required for the dehydration of glycerol at 315 °C.

The temperature-programmed desorption of NH_3 (NH_3-TPD) was carried out to probe the acidity of the support (Supplementary Figure 2). CeO_2 exhibited the well resolved desorption peaks at two distinct temperature regions. The overlapping peaks including one main peak and a shoulder were also observed over γ-Al_2O_3 and SiO_2-Al_2O_3.[32] For TiO_2 and ZrO_2, a broad TPD peak was observed. No distinguishable desorption peak of NH_3 was detected for SiO_2, AC and MgO.

The amount of desorbed ammonia and the peak position are summarized in Table 1. Based on Table 1 and the previous results,[32] the maximum TPD peak position in the low-temperature region decreased in the following order: γ-Al_2O_3 ~ ZrO_2 > TiO_2 > SiO_2-Al_2O_3 > CeO_2 ≫ SiO_2 ~ AC ~ MgO. The maximum TPD peak position in the high-temperature region decreased in the

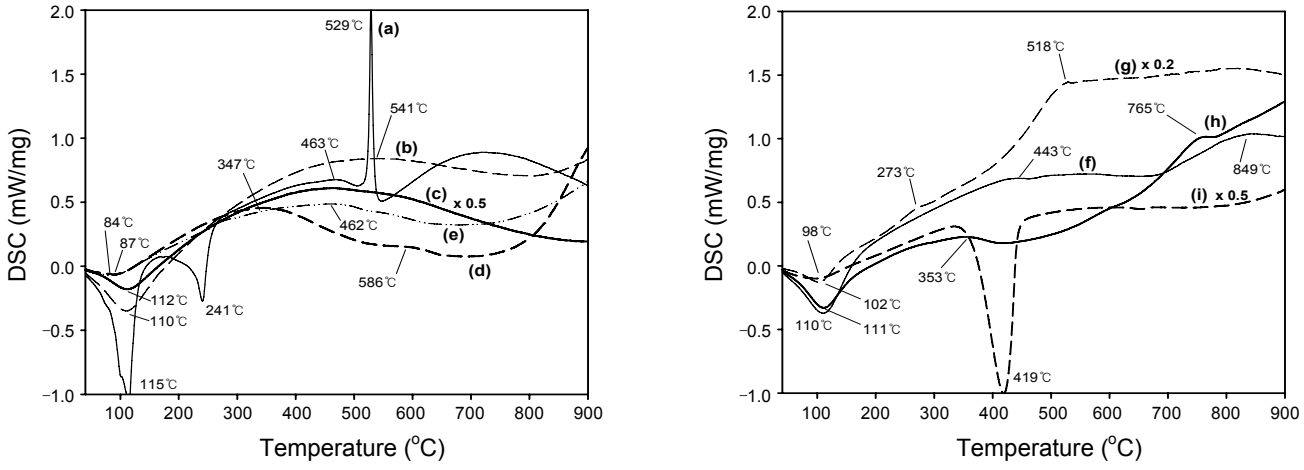

Figure 1. Variation of the heat flux with the temperature during DSC analysis for HSiW (a) and the supported HSiW catalysts, *viz*. HSiW/γ-Al_2O_3 (b) HSiW/SiO_2-Al_2O_3 (c) HSiW/TiO_2 (d) HSiW/ZrO_2 (e) HSiW/SiO_2 (f) HSiW/AC (g) HSiW/CeO_2 (h) and HSiW/MgO (i).

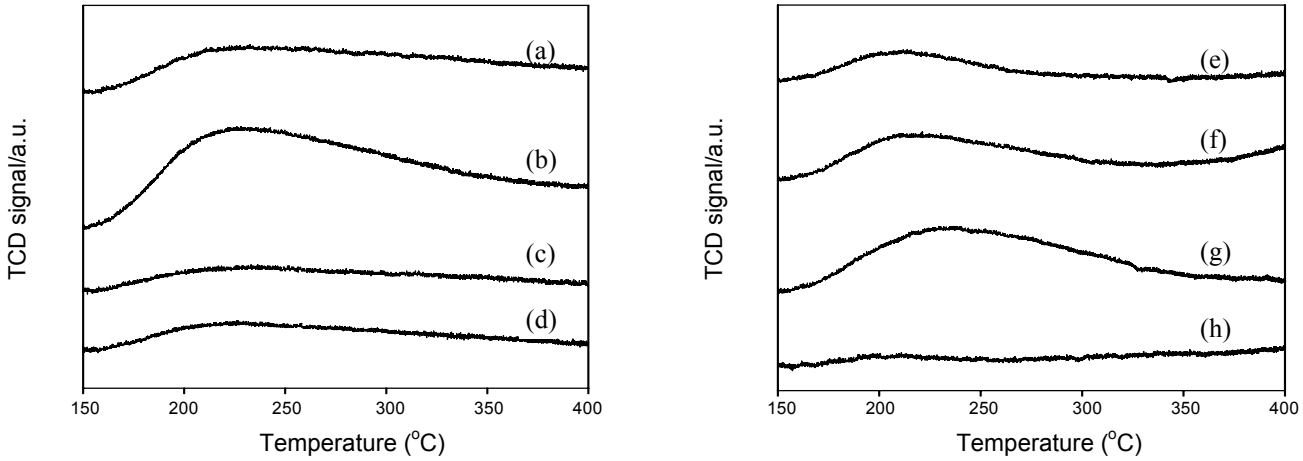

Figure 2. The temperature-programmed desorption of ammonia (NH_3-TPD) patterns of the supported HSiW catalysts, *viz*. HSiW/γ-Al_2O_3 (a), HSiW/SiO_2-Al_2O_3 (b), HSiW/TiO_2 (c), HSiW/ZrO_2 (d), HSiW/SiO_2 (e), HSiW/AC (f), HSiW/CeO_2 (g) and HSiW/MgO (h).

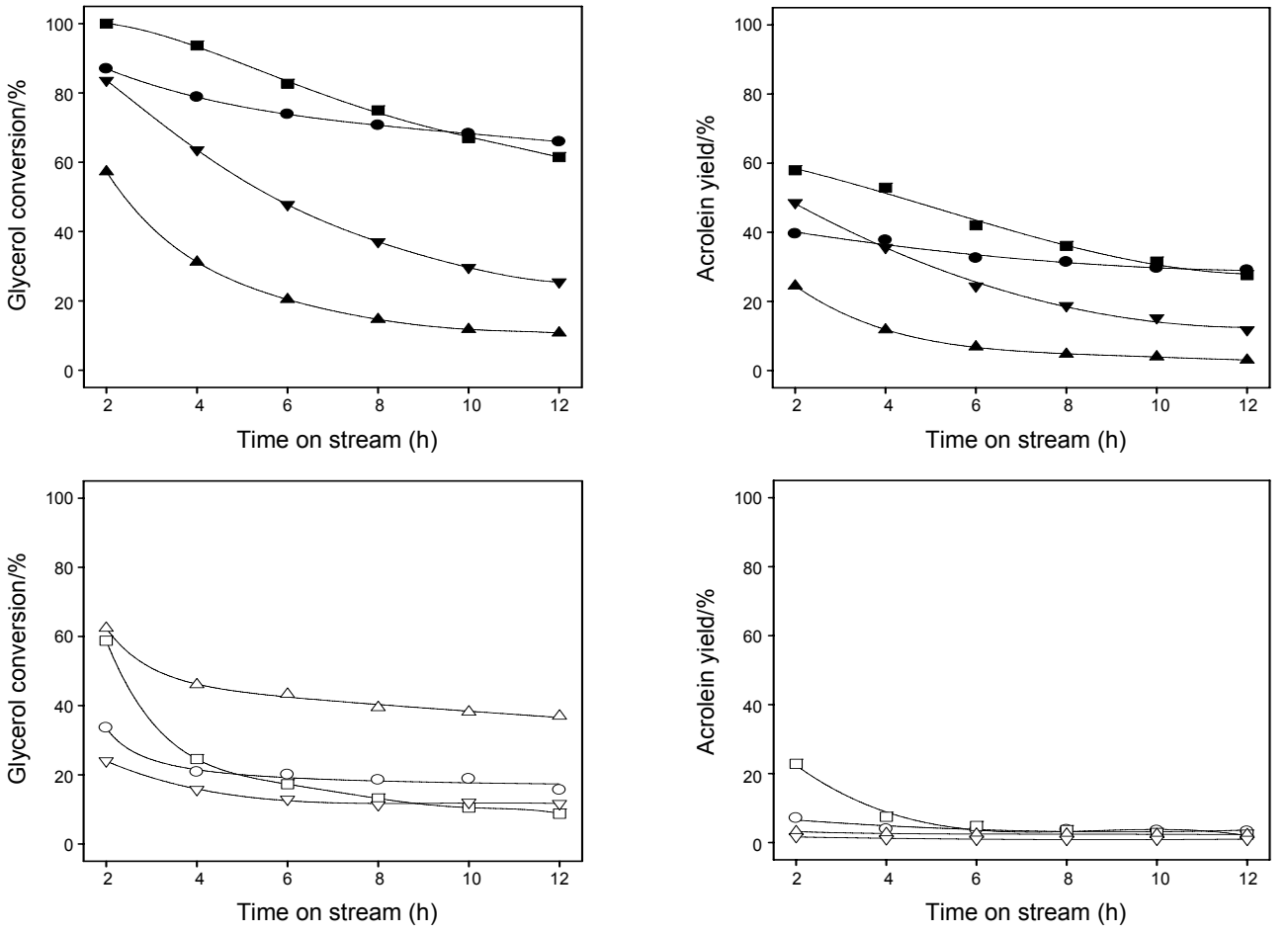

Figure 3. Variations of the glycerol conversion and acrolein yield with the time-on-stream over the supported HSiW catalysts, *viz*. HSiW/γ-Al_2O_3 (●), HSiW/SiO_2-Al_2O_3 (■), HSiW/TiO_2 (▲), HSiW/ZrO_2 (▼), HSiW/SiO_2 (○), HSiW/AC (□), HSiW/CeO_2 (△) and HSiW/MgO (▽). Feed composition: 8.3 mol % $C_3H_8O_3$, 76.3 mol % H_2O in He; T = 315 °C; Molar flow rate of glycerol = 23.4 mmol/h. Weight of the catalyst = 0.30 g.

following order: CeO_2 > γ-Al_2O_3 > SiO_2-Al_2O_3 ≫ TiO_2 ~ ZrO_2 ~ SiO_2 ~ AC ~ MgO. The total amount of acid sites decreased in the following order: SiO_2-Al_2O_3 > γ-Al_2O_3 > CeO_2 > ZrO_2 ~ TiO_2 ≫ SiO_2 ~ AC ~ MgO. Among them, SiO_2-Al_2O_3 showed the largest amount of acid sites.

NH_3-TPD was also carried out to probe the acidity of the supported HSiW catalysts, as shown in Fig. 2. As compared with the results of the corresponding support, a stronger TPD peak

Table 2. The catalytic performance for the dehydration of glycerol over the supported HSiW catalysts[a,b]

Catalyst	HSiW/γAl_2O_3	HSiW/SiO_2-Al_2O_3	HSiW/TiO_2	HSiW/ZrO_2	HSiW/SiO_2	HSiW/AC	HSiW/CeO_2	HSiW/MgO
Conversion (%)	87.0 (65.9)	100.0 (61.5)	57.3 (10.8)	83.6 (25.4)	33.6 (15.6)	58.8 (8.7)	62.4 (37.0)	24.0 (11.7)
Acrolein yield (%)	39.6 (29.0)	58.0 (27.6)	24.5 (3.0)	48.6 (11.8)	7.1 (3.3)	22.8 (2.3)	3.2 (2.3)	1.7 (0.9)
Molar carbon selectivity (%)								
Acrolein	45.5 (44.1)	58.0 (44.9)	42.8 (28.3)	58.1 (46.3)	21.1 (20.9)	38.8 (26.1)	5.1 (6.2)	7.1 (7.8)
Acetaldehyde	2.6 (2.3)	8.7 (7.4)	1.3 (0.4)	1.5 (1.4)	0.4 (0.4)	2.3 (2.5)	4.6 (4.5)	4.1 (4.8)
Allyl alcohol	1.5 (1.7)	1.0 (0.9)	1.3 (1.6)	0.7 (0.8)	0.4 (0.6)	3.3 (3.5)	4.6 (4.0)	1.0 (0.8)
1-Hydroxyacetone	13.7 (16.9)	9.6 (12.8)	5.7 (6.6)	11.9 (9.4)	4.8 (4.9)	5.5 (7.5)	23.4 (26.0)	17.0 (12.2)
Propionic acid	0.3 (0.2)	0.4 (0.3)	0.2 (0)	0.1 (0)	0.1 (0)	0.6 (0)	6.5 (4.6)	0.1 (0)
Acetone	0 (0)	0.3 (0.3)	1.4 (1.1)	0.3 (0.4)	0 (0)	0.4 (1.5)	0.9 (0.4)	0.3 (0.4)
Methanol	0.4 (0.6)	0.6 (0.9)	0 (0)	0 (0)	0 (0)	0.1 (0)	3.1 (3.9)	5.1 (5.4)
Ethanol	0.1 (0.1)	0.2 (0.1)	0 (0)	0 (0)	0 (0)	0 (0)	0.3 (0.2)	0.6 (0.4)
Others	35.9 (34.2)	21.3 (32.5)	47.4 (62.1)	27.5 (41.7)	73.3 (73.2)	49.0 (58.9)	51.6 (50.3)	64.8 (68.2)
Coke deposit[c]								
Carbon content (wt %)	11.8	23.6	11.6	10.7	12.9	-	9.7	11.2

[a]Feed composition: 8.3 mol % $C_3H_8O_3$, 76.3 mol % H_2O in He; T = 315 °C; The molar flow rate of glycerol = 23.4 mmol/h. The weight of the catalyst = 0.30g. [b]The conversion, yield, and selectivity were acquired for the products obtained during the initial 2 h of reaction. The data in parenthesis were acquired for the products obtained from 10 to 12 h of reaction. [c]After the reaction for 12 h.

was observed for the supported HSiW catalysts. For all of the supported HSiW catalysts, a new TPD peak was observed at temperatures above 400 °C where the evolution of NH_3 (m/e = 15) and H_2O (m/e = 18) was confirmed by mass spectroscopy analysis. As compared with the DSC results (Fig. 1), this implies that some NH_3 molecules strongly adsorbed on the hydrated HSiW (data not shown).

The amount of desorbed ammonia and the peak position for the supported HSiW catalysts were calculated in the temperature range below 400 °C and listed in Table 1. The maximum TPD peak position in the low-temperature region decreased in the following order: HSiW/CeO_2 ~ HSiW/γ-Al_2O_3 > HSiW/SiO_2-Al_2O_3 > HSiW/TiO_2 > HSiW/ZrO_2 > HSiW/AC > HSiW/SiO_2 ~ HSiW/MgO. The maximum TPD peak position in the high-temperature region decreased in the following order: HSiW/γ-Al_2O_3 > HSiW/SiO_2-Al_2O_3 > HSiW/TiO_2 > HSiW/ZrO_2 > HSiW/CeO_2 > HSiW/AC > HSiW/SiO_2 ≫ HSiW/MgO. The total amount of acid sites decreased in the following order: HSiW/SiO_2-Al_2O_3 > HSiW/γ-Al_2O_3 > HSiW/CeO_2 > HSiW/AC > HSiW/ZrO_2 > HSiW/TiO_2 > HSiW/SiO_2 > HSiW/MgO. The maximum TPD peak position in the low-temperature region was shifted to a lower temperature for most of the supported HSiW catalysts compared with the results of the corresponding support itself. For all of the supported HSiW catalysts, the total amount of acid sites was increased compared with that of the corresponding support excepting for HSiW/γ-Al_2O_3. In the case of HSiW/γ-Al_2O_3, the total amount of acid sites was decreased compared with that of γ-Al_2O_3. Atia *et al.* obtained similar NH_3-TPD results for HSiW/SiO_2 and HSiW/Al_2O_3. They suggested that some of the acid sites on the support were replaced with the HPAs.[21] The weak interaction between the support and heteropolyacids enables the former to keep its Brønsted acid sites which results in the increment of the acid sites, whereas the strong interaction caused the looseness of the acid sites on the support as well as the distortion of the Keggin structure.[21]

The dehydration of glycerol was examined with the time-on-stream over each support without HSiW (Supplementary Fig. 3). In our previous work,[32] the glycerol conversions obtained during the initial 2 h were 71.3 and 93.6% for γ-Al_2O_3 and SiO_2-Al_2O_3, respectively. The acrolein selectivities obtained during the initial 2 h were 36.3 and 37.8% for γ-Al_2O_3 and SiO_2-Al_2O_3, respectively. The 1-hydroxyacetone selectivities obtained during the initial 2 h were 12.7 and 9.9% for γ-Al_2O_3 and SiO_2-Al_2O_3, respectively. Therefore, the glycerol conversion obtained during the initial 2 h decreased in the following order: SiO_2-Al_2O_3 > γ-Al_2O_3 > CeO_2 > TiO_2 > MgO > ZrO_2 > SiO_2 > AC. The acrolein yield obtained during the initial 2 h decreased in the following order: SiO_2-Al_2O_3 > γ-Al_2O_3 ≫ TiO_2 > ZrO_2 > CeO_2 ~ MgO > AC > SiO_2. Among the tested metal oxides, SiO_2-Al_2O_3 showed the highest glycerol conversion and acrolein yield for all reaction times.

The product distribution from the dehydration of glycerol was obtained over each support (Supplementary Table 2). The acrolein selectivity during the initial 2 h decreased in the following order: SiO_2-Al_2O_3 > γ-Al_2O_3 > TiO_2 > ZrO_2 > AC ~ MgO > CeO_2 ~ SiO_2. As shown in Tables 1 and table (Supplementary Table 2), the glycerol conversion generally increased with increasing total amount of acid sites. Except for CeO_2, the acrolein selectivity increased with increasing maximum TPD peak position, representing the strength of the acid sites. In the case of CeO_2, strong acid sites were also observed (Supplementary Figure 2). According to the results of Hammett titration,[17] base properties ($H_o \geq +7.2$) were observed for CeO_2 and MgO. When CeO_2 and MgO were used as catalysts, the acrolein selectivity was very low. Therefore, it is clear that the basic sites are not effective for the dehydration of glycerol into acrolein, which is in good agreement with those in the literature.[17] For CeO_2, the mainly identified products were 1-hydroxyacetone and propio-

nic acid which may be formed due to the presence of acid-base pairs on CeO_2 inducing the cleavage of C-H bond.[37] Clacens *et al.* reported that polyglycerol could be synthesized with a high selectivity from glycerol over MCM-41 incorporated with basic elements.[38] Therefore, the predominant formation of polyglycerol might be one of reasons for the low acrolein selectivity over MgO which contains only basic sites. The 1-hydroxyacetone selectivity during the initial 2 h, which was the main byproduct resulting from the keto-enol tautomerism of the mono dehydrated alkoxy species, decreased in the following order: $CeO_2 > ZrO_2 > MgO > \gamma\text{-}Al_2O_3 > SiO_2\text{-}Al_2O_3 \sim TiO_2 > AC > SiO_2$. Trace of acetaldehyde, allyl alcohol, propionic acid, acetone, methanol and ethanol were detected with very low selectivities.

The dehydration of glycerol was also investigated over the supported HSiW catalysts, as shown in Fig. 3. The glycerol conversion obtained during the initial 2 h decreased in the following order: $HSiW/SiO_2\text{-}Al_2O_3 > HSiW/\gamma\text{-}Al_2O_3 > HSiW/ZrO_2 > HSiW/CeO_2 > HSiW/AC \sim HSiW/TiO_2 > HSiW/SiO_2 > HSiW/MgO$. The acrolein yield obtained during the initial 2 h decreased in the following order: $HSiW/SiO_2\text{-}Al_2O_3 > HSiW/ZrO_2 > HSiW/\gamma\text{-}Al_2O_3 > HSiW/TiO_2 > HSiW/AC > HSiW/SiO_2 > HSiW/CeO_2 > HSiW/MgO$. The supported HSiW catalysts showed superior catalytic activity to that of the corresponding support itself. Among them, $HSiW/SiO_2\text{-}Al_2O_3$ showed the highest glycerol conversion and acrolein yield. The glycerol conversion generally increased with increasing total amount of acid sites.

The product distribution results obtained from the dehydration of glycerol over the supported HSiW catalysts are listed in Table 2. The acrolein selectivity obtained during the initial 2 h decreased in the following order: $HSiW/ZrO_2 \sim HSiW/SiO_2\text{-}Al_2O_3 > HSiW/\gamma\text{-}Al_2O_3 > HSiW/TiO_2 > HSiW/AC > HSiW/SiO_2 > HSiW/MgO > HSiW/CeO_2$. Among them, $HSiW/ZrO_2$ showed the highest acrolein selectivity. Chai *et al.* suggested that the HPW Keggin structure was highly dispersed on ZrO_2 and possessed high acrolein selectivity.[22] Tsukuda *et al.* carried out the dehydration of glycerol over mesoporous silica-supported HSiW catalysts and showed that the dehydration activity increased with increasing pore diameter.[20] In the case of HSiW/AC and $HSiW/SiO_2$, significantly enhanced dehydration activity was observed because of their enhanced surface acidity compared with that of the corresponding support. However, the molar carbon selectivities for acetaldehyde, allyl alcohol, 1-hydroxyacetone, propionic acid, acetone, methanol and ethanol during the initial 2 h were not changed noticeably.

A gradual decrease in the glycerol conversion with the time-on-stream was observed for all of the tested catalysts except for TiO_2 (Supplementary Figure 3). Similar results were observed for $\gamma\text{-}Al_2O_3$ and $SiO_2\text{-}Al_2O_3$.[32] The glycerol conversion was stable with the time-on-stream over TiO_2.

The supported HSiW catalysts suffered from severe deactivation in the initial stage, as shown in Fig. 3. A linear decline in the glycerol conversion with the time-on-stream was observed over $HSiW/\gamma\text{-}Al_2O_3$. In most cases, the molar carbon selectivity for products such as acrolein, 1-hydroxyacetone and acetaldehyde did not vary with the time-on-stream.

The coke deposit on each support was analyzed by a CHNS analyzer, as summarized in table (Supplementary Table 2). The presence of crystalline carbon was not observed for any of the catalysts after the reaction based on their XRD patterns. This implies that the carbon deposited on the catalyst surface exists in the amorphous state. For $\gamma\text{-}Al_2O_3$ and $SiO_2\text{-}Al_2O_3$, the surface carbon contents (wt %) of the used catalysts were 8.6 and 18.3%, respectively.[32] Therefore, the surface carbon content (wt %) of the used catalysts decreased in the following order: $SiO_2\text{-}Al_2O_3 > CeO_2 > \gamma\text{-}Al_2O_3 > TiO_2 > MgO > SiO_2 > ZrO_2$. It is worth mentioning that the H/C ratios in the carbon formed after the reaction are high over SiO_2, MgO and ZrO_2 which have a low surface acidity. This is reasonable because the dehydration reaction can only occur on the surface acid sites, resulting in low H/C ratios.

The coke deposit on the supported HSiW catalysts was also analyzed by a CHNS analyzer, as summarized in Table 2. The

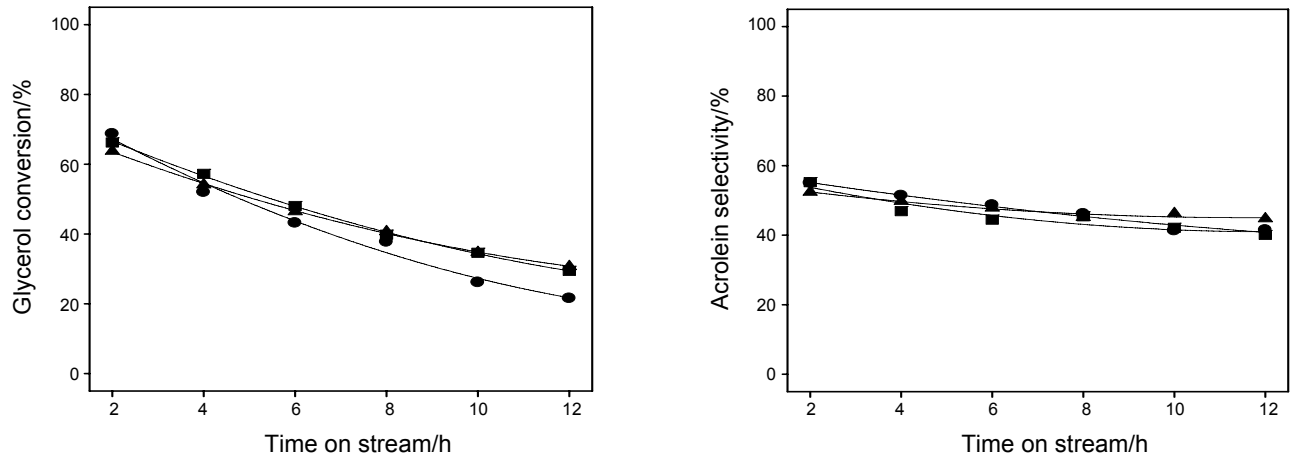

Figure 4. Variations of the glycerol conversion and acrolein selectivity with the time-on-stream over $HSiW/ZrO_2$ calcined in air at 550 °C (●), $HSiW/ZrO_2$ after the first regeneration (■), and $HSiW/ZrO_2$ after the second regeneration step (▲). Feed composition: 8.3 mol % $C_3H_8O_3$, 76.3 mol % H_2O in He; T = 315 °C; Molar flow rate of glycerol = 23.4 mmol/h. Weight of the catalyst = 0.30 g. The used catalyst was calcined in air at 550 °C for 1 h during the regeneration step.

surface carbon content (wt %) of the used catalysts decreased in the following order: HSiW/SiO_2-Al_2O_3 > HSiW/SiO_2 > HSiW/γ-Al_2O_3 ~ HSiW/TiO_2 ~ HSiW/MgO > HSiW/ZrO_2 > HSiW/CeO_2. The surface carbon content of the used HSiW/SiO_2 was high in spite of its small amount of surface acid sites. HSiW/SiO_2 has a much lower Keggin-anion density than the other catalysts tested in this work (Supplementary Table 1).

To characterize the carbon species accumulated on the catalysts, temperature-programmed oxidation (TPO) was conducted for the used catalysts (Supplementary Figure 4). The amount of carbon dioxide (m/e = 44) formed decreased in the following order: SiO_2-Al_2O_3 > CeO_2 > γ-Al_2O_3 > TiO_2 > MgO > SiO_2 > ZrO_2. Taken together, we can say that most of the maximum TPO peaks centered at a temperature below *ca*. 560 °C were observed over the metal oxides. On the other hand, TPO peaks were found at much higher temperatures over H-zeolites after the same reaction.[32] Therefore, it can be concluded that carbonaceous materials are more easily oxidized over metal oxides. Moreover, a lower TPO maximum peak position was observed over reducible metal oxides such as TiO_2, CeO_2 and ZrO_2 because of its redox properties.

In order to characterize the carbon species accumulated on the catalysts, TPO was also conducted for the supported HSiW catalysts after the reaction (Supplementary Figure 5). The amount of carbon dioxide (m/e = 44) formed decreased in the following order: HSiW/SiO_2-Al_2O_3 > HSiW/TiO_2 > HSiW/CeO_2 > HSiW/ γ-Al_2O_3 > HSiW/ZrO_2 > HSiW/SiO_2 ~ HSiW/MgO. For all of the supported HSiW catalysts, the maximum TPO peaks were shifted to higher temperatures as compared with those of the corresponding support. It is worth mentioning that the carbon formed over HSiW/ZrO_2 during the reaction can be removed in the presence of O_2 at relatively low temperatures. This implies that this catalyst can be used after the regeneration step, and since it shows excellent thermal stability, as shown in Figs. 1, the catalytic activity after the regeneration step, in which the carbon formed was burned off in an air stream at 550 °C, was examined, as shown in Fig. 4. In this case, the catalyst was calcined in air at 550 °C and then used. The amount of surface acid sites was determined to be 0.11 mmol NH_3/g_{cat}, which is smaller than that of the HSiW/ZrO_2 calcined in air at 400 °C. Therefore, the former showed lightly less catalytic activity than the latter. As shown in Fig. 4, the regenerated catalyst showed similar catalytic activity to the fresh catalyst. This implies that this catalyst can be used for continuous moving-bed reactors with a regeneration cycle.

Conclusion

Ceria showed the highest 1-hydroxyacetone selectivity during the gas-phase dehydration of glycerol at 315 °C among the various supports, *viz*. TiO_2, ZrO_2, SiO_2, AC, CeO_2 and MgO. The supported HSiW catalysts showed superior catalytic activity to the corresponding support itself. The total amount of acid sites decreased in the following order: HSiW/SiO_2-Al_2O_3 > HSiW/γ-Al_2O_3 > HSiW/CeO_2 > HSiW/AC > HSiW/ZrO_2 > HSiW/TiO_2 > HSiW/SiO_2 > HSiW/MgO. The glycerol conversion obtained during the initial 2 h decreased in the following order: HSiW/SiO_2-Al_2O_3 > HSiW/γ-Al_2O_3 > HSiW/ZrO_2 > HSiW/CeO_2 > HSiW/AC ~ HSiW/TiO_2 > HSiW/SiO_2 > HSiW/MgO. The acrolein selectivity obtained during the initial 2 h decreased in the following order: HSiW/ZrO_2 ~ HSiW/SiO_2-Al_2O_3 > HSiW/γ-Al_2O_3 > HSiW/TiO_2 > HSiW/AC > HSiW/SiO_2 > HSiW/MgO > HSiW/CeO_2. The glycerol conversion generally increased with increasing amount of acid sites. In the case of HSiW/ZrO_2, comparable catalytic activity to that of the fresh catalyst was obtained over the used catalyst after the regeneration step, in which the carbon formed was burnt off in an air stream at 550 °C.

Acknowledgments. This work was supported by the Priority Research Centers Program through the National Research Foundation of Korea (NRF) funded by the Ministry of Education, Science and Technology (2009-0094047). This work was also financially supported by a grant from the Industrial Source Technology Development Programs (10033099) of the Ministry of Knowledge Economy (MKE) of Korea.

Supporting Information. All supplementary Table 1-2 and Figure 1-5 are available *via* the Internet, http://newjournal.kcsnet.or.kr.

References

1. Pagliaro, M.; Rossi, M. *The Future of Glycerol: New Uses of a Versatile Raw Material*; The Royal Society of Chemistry: Cambridge, 2008.
2. Katryniok, B.; Paul, S.; Capron, M.; Dumeignil, F. *ChemsSusChem* **2009**, *2*, 719.
3. Bettahar, M. M.; Costentin, G.; Savary, L.; Lavalley, J. C. *Appl. Catal. A : Gen.* **1996**, *145*, 1.
4. Waldmann, H.; Petrú, F. *Chem. Ber.* **1950**, *83*, 287.
5. Groll, H. P. A. US 2,042,224 **1934**.
6. Freund, E. US 1,672,378 **1928**.
7. Hoyt, H. E.; Manninen, T. H. US 2,558,520 **1951**.
8. Schering-Kahlbaum, A. G. FR 695,931 **1930**.
9. Neher, A.; Haas, T.; Arntz, D.; Klenk, H.; Girke, W. US 5,387,720 **1995**.
10. Yang, L.; Joo, J. B.; Kim, Y. J.; Oh, S.; Kim, N. D.; Yi, J. *Korean J. Chem. Eng.* **2008**, *25*, 1014.
11. Dubois, J. L.; Duquenne, C.; Hölderich, W. US 7,396,962 **2008**.
12. Nimlos, M. R.; Blanksby, S. J.; Qian, X.; Himmel, M. E.; Johnson, D. K. *J. Phys. Chem. A* **2006**, *110*, 6145.
13. Liu, Q.; Zhang, Z.; Du, Y.; Li, J.; Yang, X. *Catal. Lett.* **2009**, *127*, 419.
14. Suprun, W.; Lutecki, M.; Haber, T.; Papp, H. *J. Mol. Catal. A: Chem.* **2009**, *309*, 71.
15. Wang, F.; Dubois, J. L.; Ueda, W. *J. Catal.* **2009**, *268*, 260.
16. Wang, F.; Dubois, J. L.; Ueda, W. *Appl. Catal. A : Gen.* **2010**, *376*, 25.
17. Chai, S. H.; Wang, H. P.; Liang, Y.; Xu, B. Q. *Green Chem.* **2007**, *9*, 1130.
18. Chai, S. H.; Wang, H. P.; Liang, Y.; Xu, B. Q. *J. Catal.* **2007**, *250*, 342.
19. Ulgen, A.; Hoelderich, W. *Catal. Lett.* **2009**, *131*, 122.
20. Tsukuda, E.; Sato, S.; Takahashi, R.; Sodesawa, T. *Catal. Commun.* **2007**, *8*, 1349.
21. Atia, H.; Armbruster, U.; Martin, A. *J. Catal.* **2008**, *258*, 71.
22. Chai, S. H.; Wang, H. P.; Liang, Y.; Xu, B. Q. *Green Chem.* **2008**, *10*, 1087.
23. Ning, L.; Ding, Y.; Chen, W.; Gong, L.; Lin, R.; Lü, Y.; Xin, Q. *Chin. J. Catal.* **2008**, *29*, 212.
24. Chai, S. H.; Wang, H. P.; Liang, Y.; Xu, B. Q. *Appl. Catal. A:*

Gen. **2009**, *353*, 213.
25. Cheng, L.; Ye, X. P. *Catal. Lett.* **2009**, *130*, 100.
26. Alhanash, A.; Kozhevnikova, E. F.; Kozhevnikov, I. V. *Appl. Catal. A : Gen.* **2010**, *378*, 11.
27. Corma, A.; Huber, G. W.; Sauvanaud, L.; O'Connor, P. *J. Catal.* **2008**, *257*, 163.
28. Yoda, E.; Ootawa, A. *Appl. Catal. A: Gen.* **2009**, *360*, 66.
29. Kim, Y. T.; Jung, K. D.; Park, E. D. *Micropor. Mesopor. Mat.* **2010**, *131*, 28.
30. Jia, C. J.; Liu, Y.; Schmidt, W.; Lu, A.-H.; Schüth, F. *J. Catal.* **2010**, *269*, 71.
31. Pathak, K.; Reddy, K. M.; Bakhshi, N. N.; Dalai, A. K. *Appl. Catal. A : Gen.* **2010**, *372*, 224.
32. Kim, Y. T.; Jung, K. D.; Park, E. D. *Appl. Catal. A : Gen.*, *submitted.*
33. Busca, G. *Chem. Rev.* **2007**, *107*, 5366.
34. Kozhevnikov, I. V. Catalysts for fine chemical synthesis volume 2 catalysis by polyoxometalates, John wiley & sons, England, 2002.
35. Kozhevnikov, I. V. *Chem. Rev.* **1998**, *98*, 171.
36. Pizzio, L. R.; Blanco, M. N. *Micropor. Mesopor. Mat.* **2007**, *103*, 40.
37. Miao, J. Y.; Yang, L. F.; Cai, J. X. *Surf. Interface Anal.* **1999**, *28*, 123.
38. Clacens, J. M.; Pouillox, Y.; Barrault, J. *Appl. Catal. A : Gen.* **2002**, *227*, 181.